Forming strengthening nanoparticles in the metal matrix of plasma deposited powder alloys coatings

D L Alontseva[1] and N V Prokhorenkova

East-Kazakhstan State Technical University, 69 Protozanov Str, Ust-Kamenogorsk, 070004, Kazakhstan

E-mail: dalontseva@mail.ru

Abstract. This paper presents the generalized results of investigation of the structure-phase compositions of thick coatings on the base of Ni and Co deposited by plasma-jet on steel substrates. Research methodology included transmission and scanning electron microscopy with energy dispersive analysis, X-ray structure phase analysis, mechanical testing. The phase structures and morphology of precipitation of strengthening nanoparticles from solid solution are defined; factor k is defined in the Hall-Petch equation for the coating materials; the coating structure model was developed. It was found that the exposure to plasma jet during the coating deposition leads to the evolution of the structural-phase state and to substantial improvement of microhardness of modified surfaces. The reason of doing this research is the necessity of the study of the structural and phase structure of these coatings and understanding what phase changes exactly are desirable in order to improve the structural behavior of the coatings at modifying treatment. Based on the experimental study, we plan to develop a scheme of the coating structure for the further use it in modeling processes taking place during additional irradiation treatment, and eventually to give evidence-based recommendations on the selection of modes of further processing.

1. Introduction

The method of plasma powder coating is a modern and promising method to deposit a coating of refractory metal materials or ceramics on various substrates [1, 2]. The formation of nanostructures in material of the coatings deposited using this method is predictable, as it is known. In particular, effective amorphous or nanocrystalline states are achieved at high heating rates, high pressure and short-term exposure to high temperatures [3]. Since coatings are deposited at high plasma temperatures, it is possible to expect the formation of a thermally stable coating, unlike nanocomposite films prepared by magnetron sputtering [4, 5].

The papers [6-10] point out that the intermetallic compounds formed in the Ni-based plasma-detonation coatings have improved corrosion resistance and strength. It is necessary to note that the carbidic strengthening phase in Ni and Co-based alloys at the temperatures of 700-800ºC coagulates much faster than the intermetallic one, which leads to quick loss of alloy strength [11]. Therefore for employing in high temperature environments the alloys with intermetallic hardening are more

[1] Address for correspondence: D L Alontseva, East-Kazakhstan State Technical University, 69 Protozanov Str, Ust-Kamenogorsk, 070004, Kazakhstan. E-mail: dalontseva@mail.ru.

preferable. Due to considerable depth of the plasma-detonation coating (100-500 μm) there is no problem of bonding of a high-duty and brittle surface film with the main material with much lower strength and high plasticity. The process of deformation takes place in a consistent structure mode through all the coating and the intermediate layer between the coating and the substrate.

Ni, Cr, and Co are the basic materials for development of solid, corrosion- and wear-resistant coatings [2, 12, 13]. As well as alloys based on Ni, the Co-based alloys can have an fcc lattice, which gives a technological advantage in comparison with the alloys based on Cr with a bcc lattice. In particular, the alloys with the fcc lattice are better welded, they retain strength at higher temperatures, are less prone to grain increase during heating, and do not lose ductility at low temperatures [12].

Some of the main problems of plasma detonated thick coatings (100-500 μm thick) are their porosity, lack of homogeneity on account of poor agglomeration of powder particles, high roughness of surface, and low adhesion to substrate. These result in insufficient corrosion and wear resistance of such coatings [1, 2]. To eliminate these drawbacks the coatings may be irradiated by electron beam in vacuum or re-treated by direct current pulse plasma jet on the surface without powder coating in air (duplex treatment). Practical experience of the use of combined technologies of coating deposition by plasma detonation with the subsequent modification by e-beam or plasma jet allows proves that the mechanical properties of such coatings of metals and alloys (microhardness, nanohardness, wear resistance, corrosion resistance) are highly desirable [2, 9, 10]. To scientifically justify the modes of additional irradiation we need to predict the structure of coatings before irradiation. There are not enough published TEM-data about the structure-phase composition of coatings deposited by plasma detonation. We need to provide the choice of duplex treatment modes according to the energy of a plasma jet or electron beam, the time of exposure of the surface, etc. Therefore we need a correct model of a structure-phase composition of a coating before additional treatment. On the basis of this model we may recommend additional irradiation modes.

One of the aims of this research is establishing structure-phase composition and mechanical properties of the plasma deposited coatings formed in result of plasma jet exposure during the coatings deposition. The other is developing a model of the coating composition on the basis of the experimental data analysis.

2. Materials and methods

An “Impulse-6” plasma detonation unit was used to form 150 -300 μm thick protective coatings of powder alloys on stainless Steel 3 substrate. For the coatings we used the Co and Ni- based powder alloys with additives of Cr: AN-35 (Co-based) and the PG-19N-01 (Ni-based). The electric current density in a plasma jet can vary from 1 to 7 A/cm^2, and the heat transmission rate in the sample varies in the q = (0.1…5) 10^6 W/cm^2 depending on the electric current density. The average temperatures of the plasma flow at the nozzle exit of the installation reach the T = (10…15) 10^3°C. The average diameter of a plasma jet on a sample is 25 mm; the pulse duration is of the order of 10 μs. Propane, oxygen and air were used as combustible and orifice gases. Mo was selected as a plasma-jet eroding electrode material. The coating was deposited and the additional treatment was produced at the Sumy Institute for Surface Modification (Sumy, Ukraine).

The experimental methods of structural-phase analysis are presented in table 1. For a more detailed analysis of the coating, it was mechanically cut off the surface of the substrate to examine the structure at different depth from the coating surface. We used the method of arbitrary secant line to define the volume fraction of phases according to the TEM-images and data [14] and CrystalMaker software to define the parameter of the crystal-lattice according to the TEM-diffraction pattern. The foils for TEM were prepared by the Ar ion sputter etching method using the Precision Ion Polishing System PIPS – M-69 (“Gatan”, USA).

The selection of the additional exposure modes is based on modeling of temperature profiles in the coatings and the substrate during irradiation. Mathematical modeling of the temperature profiles in the double-layer absorbers is described in Krasavin et al. and Alontseva et al.’s work [15-18]. We took such modes of irradiation at which the melting temperature is achieved on the surface the Ni or the Co,

and on the border between the coating and the substrate the temperature is high enough to significantly accelerate the diffusion processes and to increase the width of the diffusion zone from the coating to the substrate, but not to lead to coating melting. The optimal modes were assumed those that would lead to homogenization of the coating and improve its adhesion to the substrate due to the acceleration of diffusion processes during irradiation. Microhardness was measured at the angle laps of coatings by PMT-3 microhardness meter (LOMO, Russia) with an indentation load of 2, 5, and 10 N. We also carried out the corrosion and wearability tests as described in our work [6], however for the present research the results of microhardness tests are more important since they are directly correlated with the content of the reinforcing phases.

Table 1. The experimental methods of structural-phase analysis.

Method	Equipment	NB
X-ray diffraction (XRD)	X'Pert PRO ("PANalytical", the Netherlands)	For studying the samples' phase composition
Scanning Election Microscopy (SEM) with Energy Dispersive Spectrometry (EDS)	JSM-6390LV ("JEOL", Japan) with EDS ("Oxford Instruments", Great Britain)	The investigation of surface structure and morphology and for elemental analysis
Transmission Electron Microscopy (TEM)	JEM-2100 ("JEOL", Japan)	For studying the nanostructure

3. Results and discussion

The TEM images and microelectron-diffraction pattern surfaces confirm the presence of an amorphous layer on the surface (figure 1). The coatings have differences in the phase structure with depth. We noted the reduction of γ-phase parameter *a* in the coatings and relative increase of γ-phase peaks (220), (422), (440) intensity with depth. In general, the γ-phase peaks spread. In the coating layers that contact the substrate the volume concentration of Fe–based phases rises (Fe is the basic component of a substrate), and oxides disappear.

According to the data of the XRD the material of the substrate contains a Fe-based bcc-lattice phase (cubic, I m-3 m, 229) with the parameter *a*=2, 8662 Å.

It was proven by TEM that the base through-thickness layer of plasma detonation coatings is a mixture of crystallographically differently oriented nanograins of austenitic γ-phase (figure 2(b)) with the size of 1-2 nanometers, and lamellas of intermetallic phases up to 50 nanometers long (figures 2(a), 3(a) and 4(a)). Every indexed reflex of intermetallic phases (figures 3(b) and 4(b)) was tested by the dark field method (figures 3(c) and 4(c)).

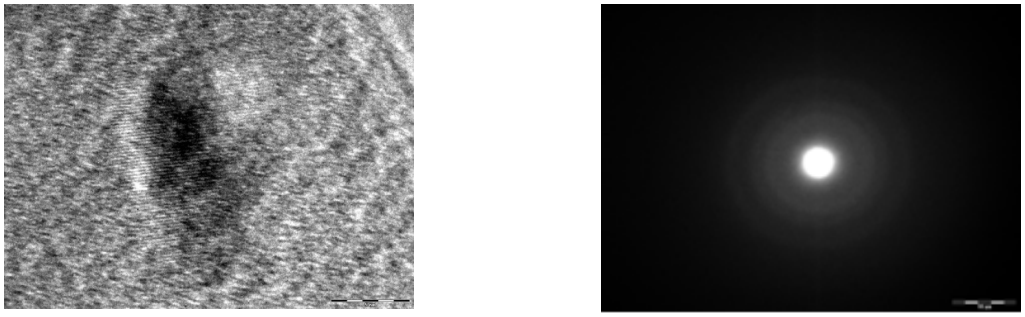

(a) (b)

Figure 1. TEM-image of the surface of AN-35 plasma-detonation coating (a); electron-diffraction pattern of the surface of AN-35 plasma-detonation coating (b).

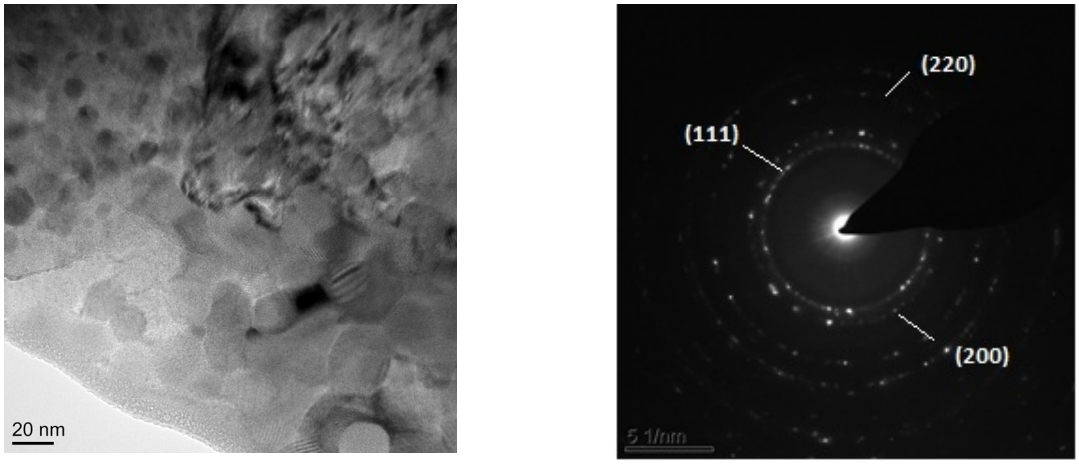

(a) (b)

Figure 2. TEM - images of PG-19N-01 powder coating deposited by plasma-detonation onto the Steel 3 substrate: the area of nanograins with different crystal-lattice orientation (a); the electron diffraction pattern of Ni-based matrix with indexes of corresponding crystallographic plates (b).

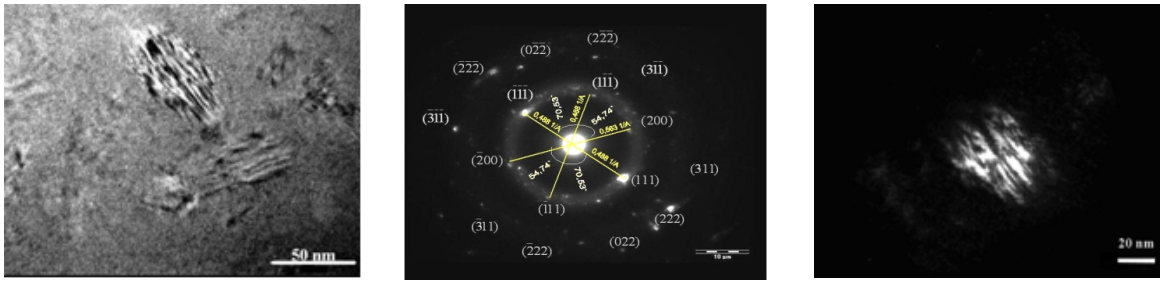

(a) (b) (c)

Figure 3. TEM - images of PG-19N-01 coating: the $CrNi_3$ particle (bright field) (a); the electron diffraction pattern of a $CrNi_3$ particle, the zone axis is $[0\bar{1}1]$ (b); the $CrNi_3$ particle (dark field) shot in point reflex (111) (c).

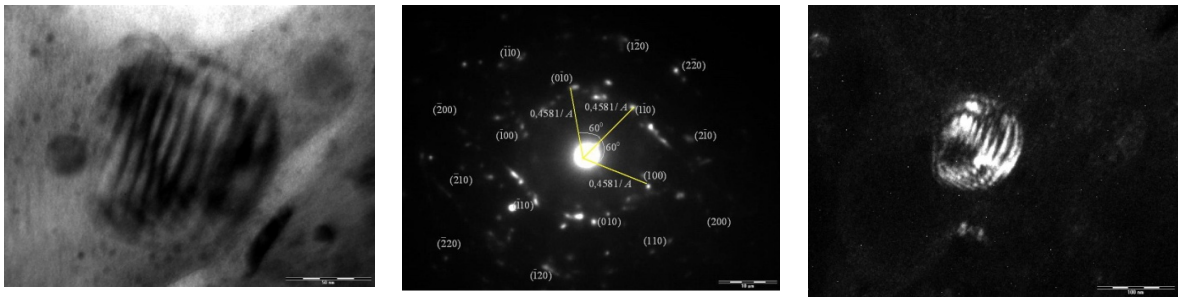

(a) (b) (c)

Figure 4. TEM - images of AN-35 coating: the $Co_{0.8}Cr_{0.2}$ particle (bright field) (a); the electron diffraction pattern of a $Co_{0.8}Cr_{0.2}$ particle, the zone axis is [001] (b); the $Co_{0.8}Cr_{0.2}$ particle (dark field) shot in point reflex $(0\bar{1}0)$ (c).

According to the XRD data the PG-19N-01 coating contains a Ni-based fcc-lattice phase with the parameter a=3.525…3.540 Å. In accordance with the estimated electron-diffraction pattern (figure 2(c)) this parameter makes 3.53 Å. The estimated fcc-lattice parameter of $CrNi_3$ (figure 3) in the coating made a= 3.58 Å (the interplane distance is 2.05 Å), which is also very close to the XRD data. The volume ratio of $CrNi_3$ in the coating PG-19N-01, as defined by TEM images, makes about 20%. In accordance with the estimated electron-diffraction pattern (figure 4(b)) the parameters of $Co_{0.8}Cr_{0.2}$ -

phase are: $a = в = 2.5$ Å and $c = 4.0$ Å. The volume ratio of $Co_{0.8}Cr_{0.2}$ in the coating AN-35, as defined by TEM images, makes about 30 %. These nanosize intermetallic phases may be called strengthening as the highest microhardness of a coating corresponds to those places where the volume concentration of these phases is highest (figure 5). Along with the microhardness measurement we measured the sizes of corresponding grains.

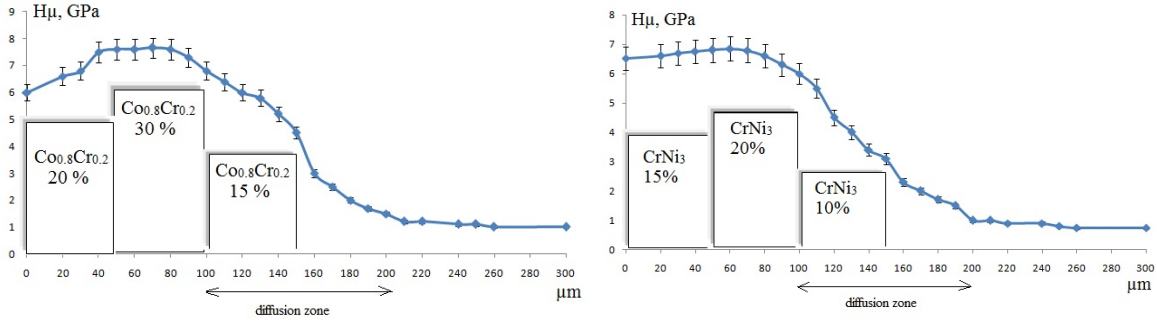

(a) (b)

Figure 5. Coating microhardness variation according to distance from the surface and to the volume concentration of intermetallic phase: AN-35 (a). Coating microhardness variation according to distance from the surface and to the volume concentration of intermetallic phase: PG-19N-01 (b).

It is particularly important that there is a transition (diffusion) zone between the coating and the substrate, where the Ni-based or Co-based γ-solid solution turns into the Fe-based solid solution with the bcc – structure, and compounds of Co or Ni with Fe evolve. The width of the diffusion zone for the samples before irradiation is estimated in average as 100 micron: 50 micron in the coating and 50 micron in the substrate (by processing the data on the distribution of microhardness across the depth from the surface, and according to the X-ray phase analysis data).

The analysis of dependence of microhardness at some distance from the surface shows that the coating microhardness is considerably higher than that of the steel substrate. The steel microhardness on the average is 1.4 GPa. The maximum microhardness of AN-35 is 8.0 GPa, and of PG-19N-01 is 7.0 GPa. It is observed in the coatings at the depth of 60 μm from the surface. The width of the transitional from a coating to a substrate layer with the increased microhardness is estimated as 100 microns, the analysis of its structurally-phase composition allows defining it as a diffusion zone.

Due to a considerable depth of the coating (150 μm) there is no problem of conjunction of high-duty and brittle surface film with the main material that possesses much lower strength and high plasticity. The process of deformation has a consistent structure rate in all the coating and the substrate intermediate layer. We think that the structure-phase state of a coating is defined by the following factors: deformational impact of a plasma jet, temperature profile distribution in the coating material, and inhomogeneous concentration of elements in the coating. The formed structures are stable at room temperature, no reduction of strength properties is observed. We explained the dependence between the linear sizes of grains and microhardness by the Hall-Petch equation (1)

$$H = H_0 + kd^{-\frac{1}{2}} \tag{1}$$

where H is microhardness, actually the strength property; k is the constant, connected with the transfer of deformation through the grain boundary; H_0 is the strain connected with the energy dissipation in motion dislocation in an infinitely large grain; d is the size of a grain. This interpretation is true because of numerous well-known empirical dependences of strength σ on hardness H; and the similar explanation of dependence was used in the paper by Musil [4] devoted to research of superhard thin films. We have defined constants in this equation for AN-35 coating: H_0=4.6GPa, k=1.4 GPaμm$^{1/2}$ and for coating PG-19N-01: H_0=4.1 GPa, k=0.6 GPaμm$^{1/2}$ for a material with the grain microstructure. If

we believe that the maximum microhardness corresponds to grains with intermetallic lamellas (figure 6), the constant k in the Hall-Petch equation will be negative for the material with the nanograin structure. Such an effect was observed by researchers in another paper by Musil [5] devoted to research of nanostructure films.

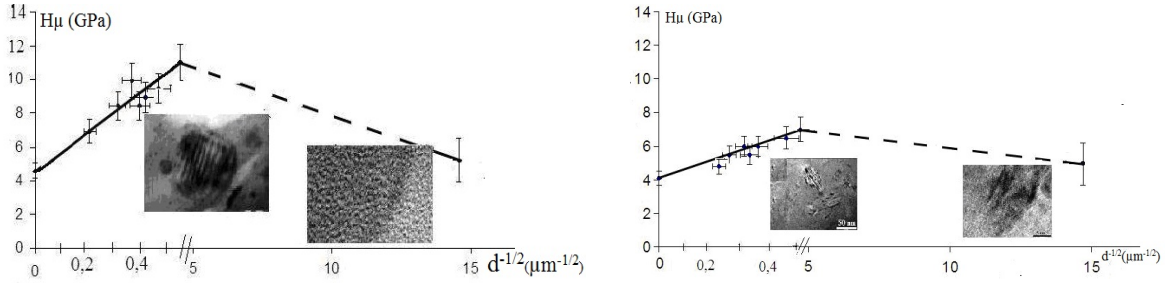

(a) (b)

Figure 6. Variation of the Hall-Petch curve trend: correlation between the grain size $d^{-1/2}$ ($\mu m^{-1/2}$) and microhardness Hμ (GPa) for coating AN-35 (a) and for coating PG-19N-01 (b).

We consider that the nanocrystalline patterns found in these coatings are distinctive for all the coatings deposited by the plasma detonation method, and partially characteristic for the substrate layer next to the coating. Some of the reasons are high micro structure defectiveness conditioned by the plasma jet impact action on the surface and steep temperature gradient in the coating, which may lead to a great deformation in a coating. As a result, in order to remove the strains in a coating there is formed a substructure of nanograins of different crystal lattice orientation with high and continuous disorientation, which is proved by distinctive ring electron-diffraction patterns. When the foils in a goniometer are oriented randomly, there are no characteristics of polycrystals features of diffraction contrast, namely, the changes of its intensiveness on the boundaries necessary for defining grain edges. We assume that we observe the pattern similar to the one of crystal polygonization that is a fragmented pattern with fragments being disoriented nanograins. The validation of this assumption for the coatings lies in some diffusion of the peaks and lowering of their intensiveness in the X-Ray diffractograms. Though in electron diffraction pattern all the reflexes of face-centered cubic lattice are observed, the planes with the axis <111> zone give brighter reflexes (figure 7(a)). It is indicative of fiber texture (figure 7(b)). The axis of the fiber texture is perpendicular to the coating surface along the heat current which develops at heating and the subsequent cooling of the coating during deposition by a plasma jet. Next to the substrate layer the coatings are deformed (figure 7(c)). Basing on the results of research of microstructure, the phase structure, and microhardness of plasma detonation coatings at depth from the surface, we developed the scheme of the coating structure (figure 8). This scheme was used at working out the model of the temperature profile distribution in these coating under irradiation by a plasma jet or an e-beam.

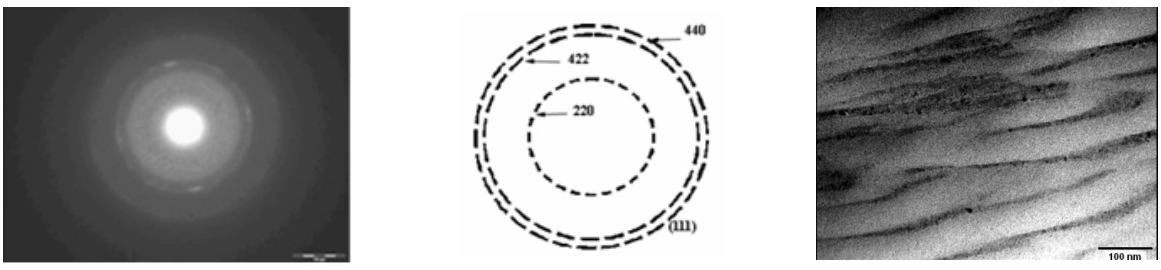

(a) (b) (c)

Figure 7. The electron-diffraction pattern of AN-35 coating with the texture with an axis type <111> zone (a) and (b); the defects in a contact layer of coating PG-19N-01with substrate (c).

The temperature interval of $CrNi_3$-phase in Ni-Cr solid solution (Cr 20-40 at.%) is 500-600°C according to the data of Nash [19]; the existence of the temperature interval of the $Co_{0.8}Cr_{0.2}$ phase is not specified in references. Blake et al. [20] note the existence of an intermediate $CrCo_3$–phase in the Fe-Co system. But the temperature intervals of the advent of phases in a non-equilibrium open system, like an irradiated and complex in structure coating, may not coincide with the data of equilibrium phase diagrams.

The formation of phases on the Cr basis caused some concern because of the known effect of embrittlement of austenite materials at chromiferrous phase precipitation on the boundaries of austenitic grains (σ - a phase with a tetragonal lattice or carbides) [21]. On the other hand, austenite alloys with high Cr content are known for the effect of their hardening by disperse intermetallic γ'-phase (fcc) or η – phase (hcp) due to the mechanism of cellular precipitation [22]. In case of our investigation it is obvious that precipitation of disperse nanosized lamellas of intermetallic compounds raises coating durability; the highest microhardness is observed in those layers of coatings where the volume fraction of intermetallic compounds is maximal (see figure 5).

The scheme of the structure of coatings on Ni - Cr and Co–Cr based powder alloys deposited by plasma-detonation on the steel substrates is presented in figure 8. Figure 8(a) displays the nanograins and intermetallic phase precipitation with their electron diffraction pattern, where: 1- amorphous layer with oxides and carbides; 2-textured layer (solid solution on Co-base with intermetallic phase) and unmelted particles of coating powder; 3-intermediate coating layer (coating-substrate) with deformed and broken particles of coating; 4-intermediate substrate layer with fine-grained microstructure; 5-substrate with large grains. The strokes show precipitations of lamellas of intermetallic phase.

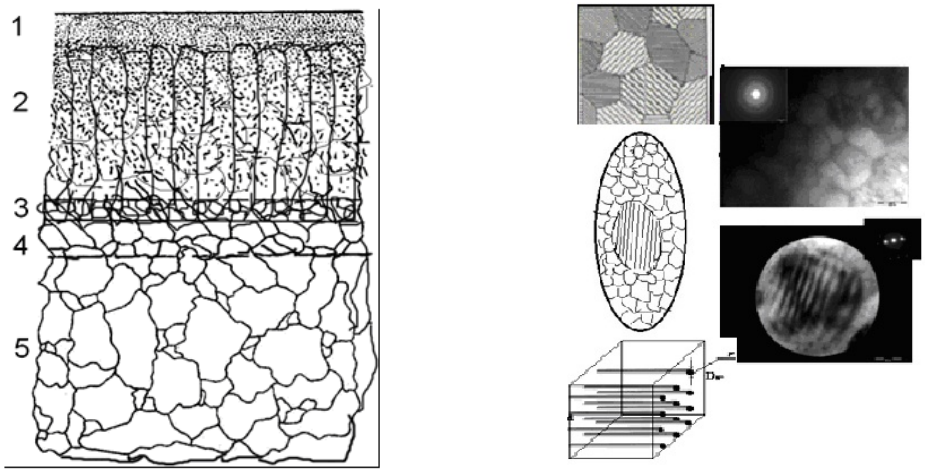

(a) (b)

Figure 8. The scheme of the structure of the Ni - Cr and Co–Cr based powder alloy coatings deposited by plasma-detonation on the steel substrates (a) the scheme of nanograin structure and the scheme of cubic grain with lamellas of an intermetallic phase, and their TEM – images with corresponding electron diffraction patterns (b).

The coatings need additional irradiation for reduction of surface roughness and the increase of their homogeneity. On the basis of the experimental structural and phase analysis of coating microstructure we developed the model of structure for plasma-detonation deposited Co and a Ni- based coating. The applied value of the model was used to calculate the mode of additional irradiation for modifying the coatings.

4. Conclusions

The study of the features of the plasma-deposited powder Ni and Co-based coatings allowed establishing their structural-phase composition and define the phase structures and morphology of precipitation of strengthening nanoparticles from solid solution. Factor k was defined in the Hall-Petch

equation for the coating materials. The authors developed the model of structure for the coatings. It was found that the exposure of plasma jet during the coatings deposition leads to the evolution of the structural-phase state and substantial improvement of performance properties of modified surfaces. The authors also identified the mechanism of surface improvement. In general the structure-phase changes are represented by the forming of nanosized intermetallic phase volume concentration and existing of the diffuse zone in the coating layer contacting the substrate.

Acknowledgments
This research is funded by the Scientific Committee of the Ministry of Education and Science of the Republic of Kazakhstan for the project No 29-417-15 “Automated precision deposition of powder coating multifunctional systems”.

References
[1] Misaelides P, Hatzidimitou A, Noli F, Pogrebnjak A, Tyurin Yu N and Kosionidis S 2004 Preparation, characterization and corrosion behavior of protection coatings on stainless steel deposited by plasma detonation *Surface and Coatings Technology* **180-181** 290-6
[2] Kadyrzhanov K, Komarov F, Pogrebnyak A, Russakov V and Turkebaev T 2005 *Ion-Beam and Ion-Plasma Modification of Materials* (Moscow: Moscow State University) p 640
[3] Poate J, Foti G and Jacobson D 1983 *Surface Modification and Alloying by Laser, Ion, and Electron Beams* (New York, USA) p 424
[4] Musil J 2000 Hard and superhard nanocomposite coatings *Surface and Coatings Technology* **125** 322-30
[5] Musil J 2005 *Physical and Mechanical Properties of Hard Nanocomposite Films Prepared by Reactive Magnetron Sputtering* (NewYork: Nanostructured Hard Coating*)* chapter 10 pp 407-63
[6] Alontseva D, Bratushka S, Il'yashenko M, Makhmudov N, Prokhorenkova N, Onanchenko E, Novgorodtsev A and Rogoz V 2012 Formation of stable nanostructured phases in plasma-jet-treated Ni-Cr powder coating *Physics of Metals and Metallography* **113** 785-94
[7] Alontseva D and Russakova A 2013 The structure-phase compositions and properties of plasma-detonation Ni and Co-based powder alloys coatings *Advanced Materials Research* **702** 94-9
[8] Alontseva D, Missevra S and Russakova A 2013 Characteristics of structure and properties of plasma-detonated Ni-Cr and Co-Cr based powder alloys coatings *Journal of Materials Science and Engineering* **3** 41-9
[9] Alontseva D, Pogrebnjak A, Kolesnikova T and Russakova A 2013 Modeling of processes in Co-based coatings exposed to plasma jet irradiation *Medziagotyra* **19** 277-82
[10] Alontseva D, Krasavin A, Pogrebnjak A and Russakova A 2013 Modification of Ni-based plasma detonation coatings by a low-energy DC E-Beam *Acta Physica Polonica A* **123** 867-70
[11] Hassanein A, Kulsinski G and Wolfer W 1981 Vaporization and melting of materials in fusion devices *Journal of Nuclear Materials* **103 -104** 321-6
[12] Burns R and Bradley W 1967 *Protective Coatings for Metals* (New York, USA) p 735
[13] Elsea A, Westerman A and Manning G 1949 The Co-Cr binary system *Trans. AIME Metals Technology* **180** 579
[14] Egerton R F 2010 *Physical Principles of Electron Microscopy. An Introduction to TEM, SEM and AFM* (Moscow) p 304
[15] Krasavin A, Alontseva D and Denisova N 2013 *Certificate of Authorship No. 0010558 of the Republic of Kazakhstan for the Computer Program*
[16] Alontseva D, Krasavin A, Kolesnikova T and Russakova A 2012 Computer simulation of temperature profiles of a two-layer sample during heating by the electron beam *Proceedings of the 7th International Symposium on Applied Informatics and Related Areas (AIS)* 53-56
[17] Alontseva D, Krasavin A, Russakova A and Sadvakasova N 2013 Computer simulation of temperature profiles for DC pulse plasma jet modification of Co-based plasma detonation

coatings *Scientific Journal Proceedings of the International Conference Nanomaterials: Applications and Properties* **2** 11-4
[18] Alontseva D, Krasavin A, Russakova A and Bektasova G 2014 Modeling of irradiation induced processes of heat transfer in bilayer metal absorbers *Materials of 5th International Conference "Radiation Interaction with Materials: Fundamentals and Applications*" 210-213
[19] Nash P 1986 The Cr–Ni (Chromium–Nickel) system *Bulletin of Alloy Phase Diagrams* **27** 466-7
[20] Blake F, Lord J and Focke A 1987 Solid solution of chromium in nickel and of iron in nickel *Physical Revew 2nd Series* **29** 206-7
[21] Naohara T 1983 The formation of s-phase in binary alloys *Scr. Met* **17** 111-4
[22] Sukhovarov V F 1983 *The Cellular Precipitation in Alloys* (Novosibirsk: Nauka) p 164